Means, G. E., & Feeney, R. E. (1971) *Chemical Modifications of Proteins*, p 222, Holden-Day, Inc., San Francisco, CA.
Mumby, S. M., Casey, P. J., Gilman, A. G., Gutowski, S., & Sternweis, P. C. (1990) *Proc. Natl. Acad. Sci. U.S.A. 87*, 5873-5877.
Munemitsu, S., Innis, M. A., Clark, R., McCormick, F., Ullrich, A., & Polakis, P. (1990) *Mol. Cell. Biol. 10*, 5977-5982.
Murray, E. D., Jr., & Clarke, S. (1984) *J. Biol. Chem. 259*, 10722-10732.
Perez-Sala, D., Tan, E. W., Canada, F. J., & Rando, R. R. (1991) *Proc. Natl. Acad. Sci. U.S.A. 88*, 3043-3046.
Rando, R. R. (1974) *Science 185*, 320-324.
Reiss, Y., Goldstein, J. L., Seabra, M. C., Casey, P. J., & Brown, M. S. (1990) *Cell 62*, 81-88.
Reiss, Y., Stradley, S. J., Gierasch, L. M., Brown, M. S., & Goldstein, J. L. (1991) *Proc. Natl. Acad. Sci. U.S.A. 88*, 732-736.
Rilling, H. C., Breunger, E., Epstein, W. W., & Crain, P. F. (1990) *Science 247*, 318-320.
Schaber, M. D., O'Hara, M. B., Garsky, W. M., Mosser, S. D., Bergstrom, J. D., Moores, S. L., Marshall, M. S., Friedman, P. A., Dixon, R. A. F., & Gibbs, J. B. (1990) *J. Biol. Chem. 265*, 14701-14704.
Schafer, W. R., Kim, R., Sterne, R., Thorner, J., Kim, S.-H., & Rine, J. (1989) *Science 245*, 379-385.
Seabra, M. C., Reiss, Y., Casey, P. J., Brown, M. S., & Goldstein, J. L. (1991) *Cell 65*, 429-434.
Shinjo, K., Koland, J. G., Hart, M. J., Narasimhan, V., Johnson, D. I., Evans, T., & Cerione, R. A. (1990) *Proc. Natl. Acad. Sci. U.S.A. 87*, 9853-9857.
Simonds, W. F., Butrynski, J. E., Gautami, N., Unson, C. G., & Spiegel, A. M. (1991) *J. Biol. Chem. 266*, 5363-5366.
Springer, M. S., Goy, M. F., & Adler, J. (1979) *Nature 280*, 279-284.
Stephenson, R. C., & Clarke, S. (1990) *J. Biol. Chem. 265*, 16248-16254.
Swanson, R. J., & Applebury, M. L. (1983) *J. Biol. Chem. 258*, 10599-10605.
Tan, E. W., Perez-Sala, D., Canada, F. J., & Rando, R. R. (1991a) *J. Am. Chem. Soc. 113*, 6299-6300.
Tan, E. W., Perez-Sala, D., Canada, F. J., & Rando, R. R. (1991b) *J. Biol. Chem. 266*, 10719-10722.
Taylor, B. L., & Panasenko, S. M. (1984) *Membranes and Sensory Transduction* (Colombetti, G., & Lenci, F., Eds.) Plenum Press, New York.
Umezawa, H., Aoyagi, T., Uotani, K., Hamada, M., Takeuchi, T., & Takahashi, S. (1980) *J. Antibiot. 33*, 1594-1596.
Waxman, D. J., & Stominger, J. L. (1983) *Annu. Rev. Biochem. 52*, 825-869.
Yamane, H. K., Farnsworth, C. C., Xie, H., Howald, W., Fung, B. K.-K., Clarke, S., Gelb, M. H., & Glomset, J. A. (1990) *Proc. Natl. Acad. Sci. U.S.A. 87*, 5868-5872.
Yamane, H. K., Farnsworth, C. C., Xie, H., Evans, T., Howald, W. N., Gelb, M. H., Glomset, J. A., Clarke, S., & Fung, B. K.-K. (1991) *Proc. Natl. Acad. Sci. U.S.A. 88*, 286-290.

The Secondary Structure of the Colicin E3 Immunity Protein As Studied by ^1H-^1H and ^1H-^{15}N Two-Dimensional NMR Spectroscopy†

Shunsuke Yajima,‡ Yutaka Muto,§ Shigeyuki Yokoyama,§ Haruhiko Masaki,*,‡ and Takeshi Uozumi‡
Department of Biotechnology, Faculty of Agriculture, and Department of Biophysics and Biochemistry, The University of Tokyo, Bunkyo-ku, Tokyo 113, Japan

Received January 21, 1992; Revised Manuscript Received March 31, 1992

ABSTRACT: By performing ^1H-^1H and ^1H-^{15}N two-dimensional (2D) nuclear magnetic resonance (NMR) experiments, the complete sequence-specific resonance assignment was determined for the colicin E3 immunity protein (84 residues; ImmE3), which binds to colicin E3 and inhibits its RNase activity. First, the fingerprint region of the spectrum was analyzed by homonuclear ^1H-^1H HOHAHA and NOESY methods. For the identification of overlapping resonances, heteronuclear ^1H-^{15}N (HMQC-HOHAHA, HMQC-NOESY) experiments were performed, so that the complete ^1H and ^{15}N resonance assignments were provided. Then the secondary structure of ImmE3 was determined by examination of characteristic patterns of sequential backbone proton NOEs in combination with measurement of exchange rates of amide protons and $^3J_{HN\alpha}$ coupling constants. From these results, it was concluded that ImmE3 contains a four-stranded antiparallel β-sheet (residues 2-10, 19-22, 47-49, and 71-79) and a short α-helix (residues 31-36).

Colicin E3 is an antibacterial protein (551 residues) which kills sensitive *Escherichia coli* cells through binding to a common outer membrane receptor, BtuB (Pusgley & Oudega, 1987). E3 is a special kind of RNase which inactivates 16S RNA of 70S ribosomes, and this activity is exclusively defined by the C-terminal T2A domain of E3 (Boon, 1971; Bowman et al., 1971; Suzuki & Imahori, 1978; Ohno-Iwashita & Imahori, 1980). E3 is encoded by an *E. coli* plasmid, ColE3. The plasmid protects the host cell from both exogenous and endogenous colicin actions, a phenomenon referred to as immunity, by synthesizing the immunity protein (Imm), which specifically binds to the T2A domain and inhibits its RNase activity (Jakes & Zinder, 1974; Mochitate et al., 1981; Masaki & Ohta, 1985).

ColE6-directed colicin E6 is an E3 homologue, and the sequence differences of the two are almost confined in their

† This work was supported by Grants-in-Aid from the Ministry of Education, Science and Culture of Japan.
* Corresponding author.
‡ Department of Biotechnology, The University of Tokyo.
§ Department of Biophysics and Biochemistry, The University of Tokyo.

0006-2960/92/0431-5578$03.00/0

T2A domains, as well as cognate Imm proteins, reflecting different immunity specificities. On the other hand, plasmid CloDF13-directed cloacin DF13 has a different in vivo killing spectrum from colicins but exhibits almost the same in vitro activity as E3 toward ribosomes (de Graaf et al., 1973) and also shows a completely identical immunity specificity to E6, but not E3. These structural and functional comparison of E3, E6, and DF13 restricted the possible specificity determinants of immunity into eight of 97 amino acid residues in T2A domains and nine of 84 residues in Imm proteins (Akutsu et al., 1989).

Furthermore, our genetic study identified Cys-47 as the major specificity determinant of ImmE3 and also suggested that Glu-19 is a subdeterminant of ImmE3 and His-5 and Trp-47 of Imm6 are essential to its immunity specificity (Masaki et al., 1991).

While T2A domains share an enzymatic function, the immunity specificities are entirely different, suggesting that the Imm proteins recognize the amino acids of the T2A domain other than those forming the enzymatic active sites, possibly those on the surface of the T2A domain. The situation is quite different from the case of a protease and its protein inhibitor, in which the inhibitor can be regarded as a nondigestible substrate analogue. We believe that the T2A domain and the Imm protein forming a small heterodimer represent a promising model system which allows us to study protein–protein interactions both genetically and physicochemically.

In recent years, the advanced NMR[1] techniques have enabled us to determine a protein structure whose molecular mass is up to about 20 kDa (Torchia et al., 1989; Arrowsmith et al., 1990; Driscoll et al., 1990; Ikura et al., 1990; MacIntosh et al., 1990; Wang et al., 1990; Dekker et al., 1991; Fairbrother et al., 1991; Yamasaki et al., 1992). And the NMR techniques, especially stable isotopic labeling techniques, are also suitable for elucidation of the local and global dynamic properties of a protein in aqueous solution. These features in NMR spectroscopy provide useful information on studying the higher-order structures of the T2A domain and Imm, which have not been known, and, moreover, the mechanism of the interaction of the T2A domain with Imm in solution.

We therefore started an NMR study with the aim of determining the three-dimensional structure of the ImmE3 protein. In this paper, we report the assignment of both the ^1H and ^{15}N NMR resonances of the ImmE3 protein and the elucidation of its secondary structure by using conventional 2D NMR experiments, DQF-COSY, HOHAHA, and NOESY, in combination with ^1H–^{15}N heteronuclear 2D NMR experiments, HMQC, HMQC-HOHAHA, and HMQC-NOESY.

Materials and Methods

Bacterial Strains. *E. coli* K12 W3110 was used as the host strain of plasmids. Plasmid pUIE3 is a pUC18 (Messing, 1983; Yanisch-Perron et al., 1985) derivative containing the 298 bp *Sau3*AI fragment (*immE3*) of ColE3 (Masaki & Ohta, 1985) under the control of the *lac* promoter, which was induced with 0.2 mM isopropyl β-D-thiogalactopyranoside. Plasmid pSH312 carries an SOS-responsive colicin operon including *colE3* and *immE3* genes (Toba et al., 1986), whose expression was induced with 0.5 mg/mL mitomycin C.

Protein Purification. For the nonlabeled protein preparation, the W3110 (pUIE3) cells were grown in 1 L of L-broth, harvested, and disrupted by ultrasonication in 20 mM potassium phosphate buffer, pH 7.5. After centrifugation, the supernatant was applied to a DEAE-Toyopearl 650S (Tosoh Corp.) column and eluted with a linear gradient of 0.0–0.5 M KCl in the same buffer, followed by application to a Mono-Q HR 10/10 (Pharmacia LKB Biotechnology Inc.) column with the same gradient as in the case of a DEAE-Toyopearl. About 8 mg of ImmE3 protein was obtained from the initial 10 g of wet cells.

For the uniformly ^{15}N-labeled protein preparation, the W3110 (pSH312) cells were grown in 5 L of M9 minimal medium containing $^{15}NH_4Cl$ as the sole nitrogen source. The harvested cells were disrupted by ultrasonication in 20 mM potassium phosphate buffer, pH 7.5, containing 1 M $(NH_4)_2SO_4$. After centrifugation, the supernatant was applied to a Phenyl-Toyopearl 650M (Tosoh Corp.) column and eluted with a decreasing linear gradient of 1.0–0.0 M $(NH_4)_2SO_4$ in 20 mM potassium phosphate buffer, pH 7.5. After dialysis against the same buffer, the protein was applied to a DEAE-Toyopearl 650S column and recovered from the flow-through fraction. After the dialysis against 20 mM potassium phosphate buffer, pH 6.0, the sample was applied to an S-Sepharose (Pharmacia LKB Biotechnology Inc.) column and eluted with a linear gradient of 0.0–0.5 M KCl in the same buffer. The purified E3–ImmE3 complex was dissolved with 6 M urea in 20 mM potassium phosphate buffer, pH 7.5, and ImmE3 was purified through a Mono-Q 10/10 column in a linear gradient of 0.0–0.5 M KCl in the same buffer. About 8 mg of the ^{15}N-labeled ImmE3 protein was obtained from the initial 20 g of wet cells.

Sample Preparation. For the NMR experiments, the purified ImmE3 samples were dialyzed against 20 mM potassium phosphate buffer, pH 6.0, containing 100 mM KCl, and then against the same buffer with 90% ^1H_2O/10% ^2H_2O. For the experiment in ^2H_2O/^1H_2O, the sample buffer was exchanged for the same buffer containing 99.96% ^2H_2O by ultrafiltration using Centricon-3 (Amicon Division, W. R. Grace & Co.). The pH value of the sample was measured at 23 °C and adjusted with small amount of ^2HCl. Sample concentration was 4 mM in all experiments.

NMR Spectroscopy. NMR measurements were carried out on a 600-MHz Bruker AM-600 spectrometer with an Aspect 3000 computer. All two-dimensional spectra were recorded in the pure phase absorption mode by using the time-proportional phase incrementation method (Redfield & Kunz, 1975; Marion & Wüthrich, 1983) at 30 °C and pH 6.0. Dimethylsilylsulfonic acid (DSS) was used as internal reference at 0 ppm for ^1H. For ^{15}N chemical shift assignments, a value of 0 ppm for NH_4^+ was used. The resonance frequency of NH_4^+ was established by ^{15}N detection of a sample that was 2.9 M $^{15}NH_4Cl$ in 1.0 M HCl.

NOESY spectra (Jeener et al., 1979; Macura et al., 1981) with mixing times of 80 and 150 ms, HOHAHA spectra (Braunschweiler & Ernst, 1983; Davis & Bax, 1985) with MLEV-17 mixing sequences (Bax & Davis, 1985) of 30–90 ms, and DQF-COSY spectra (Piantini et al., 1982; Rance et al., 1983) were recorded with a spectral width of 9615 Hz in the F_2 dimension.

For NOESY and HOHAHA spectra recorded in ^1H_2O, the water resonance was suppressed by presaturation during the relaxation delay and, in the case of the NOESY experiments, during the mixing time as well. For the observation of the

[1] Abbreviations: NMR, nuclear magnetic resonance; NOE, nuclear Overhauser effect; NOESY, two-dimensional nuclear Overhauser enhancement spectroscopy; DQF-COSY, two-dimensional double-quantum filtered correlated spectroscopy; HOHAHA, two-dimensional homonuclear Hartmann–Hahn spectroscopy; HMQC, two-dimensional heteronuclear multiple-quantum correlated spectroscopy.

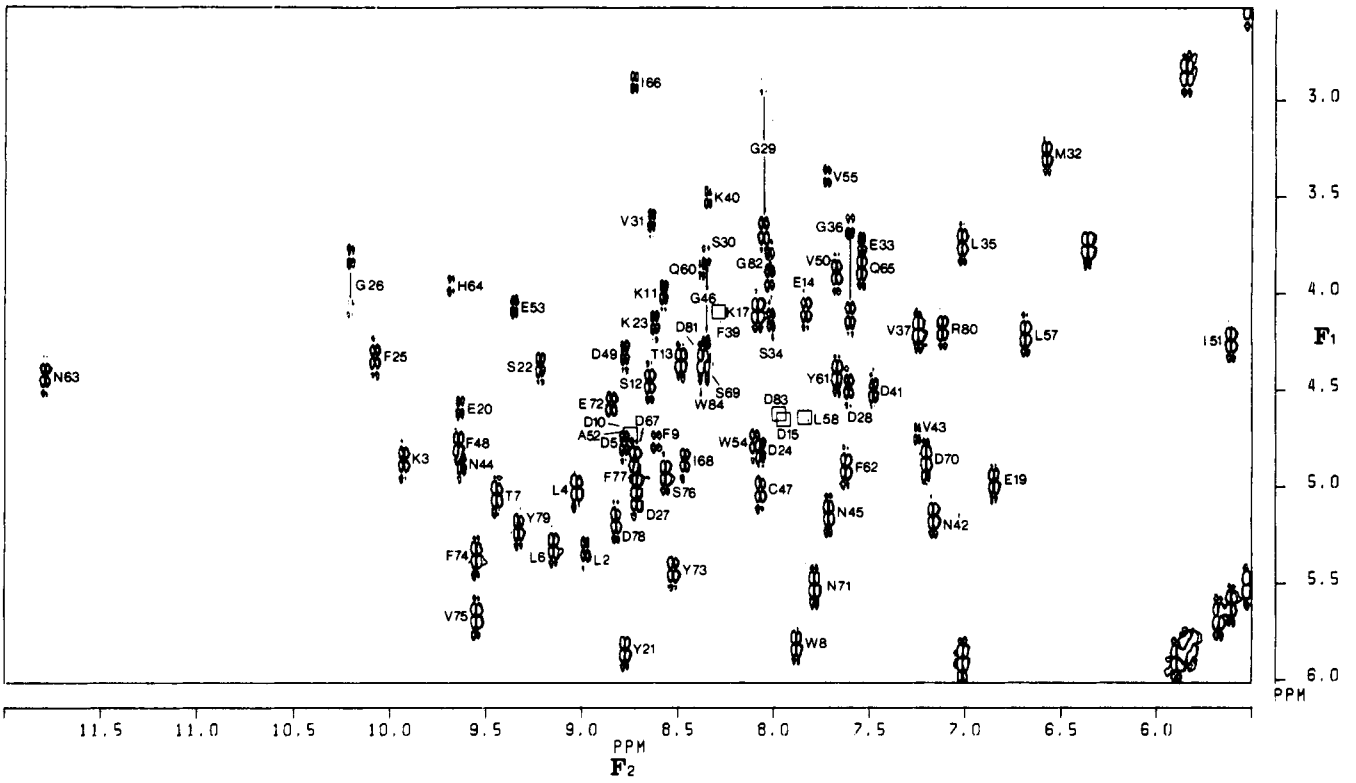

FIGURE 1: Fingerprint region of the DQF-COSY spectrum of the ImmE3 protein in ^1H_2O, at pH 6.0 and 30 °C. The boxes indicate the positions of the cross peaks identified by the HOHAHA spectra in ^1H_2O or by the HMQC-HOHAHA spectra.

resonances bleached by the presaturation of the water resonance, a "jump-and-return" pulse was used in place of the last 90° pulse in the NOESY sequence (Plateau & Gueron, 1982), and a 90° "flip-back" pulse followed by a jump-and-return pulse after the MLEV-17 mixing sequence in the HOHAHA measurements (Bax et al., 1987).

Typically, a total of 400–512 increments of 2K data points were collected for each ^1H–^1H 2D NMR experiment, resulting in a 2D spectrum with a digital resolution of 4.7 Hz/point in both dimensions after zero-filling.

^1H–^{15}N HMQC spectra (Mueller, 1979; Redfield, 1983; Bax et al., 1983; Sklenar & Bax, 1987; Glushka & Cowburn, 1987), ^1H–^{15}N 2D HMQC-NOESY spectra (Gronenborn et al., 1989) with a mixing time of 100 ms, and ^1H–^{15}N 2D HMQC-HOHAHA spectra with an MLEV-17 mixing sequence of 40 ms were recorded with spectral widths of 9615 and 2016 Hz in the ^1H and ^{15}N dimensions, respectively. A total of 512 increments of 2K data were collected for each spectrum. Water suppression was achieved by presaturation as well as in the NOESY and HOHAHA measurements. The digital resolution for those spectra was 7.9 Hz/point in F_1 and 4.7 Hz/point in F_2 after zero-filling in each dimension.

All spectra except HMQC-J spectra were processed with square sine bell window functions shifted by $\pi/8$ in the F_1 dimension and $\pi/4$ in the F_2 dimension.

HMQC-J spectra (Kay & Bax, 1990) was recorded with 2K data points in F_2 and 1024 increments in F_1 with a spectral width of 4807.7 Hz. Spectra were zero-filled to give 4K data points, resulting in the digital resolution of 1.0 Hz/point in the F_1 dimension, and the values of the $^3J_{NH\alpha}$ coupling constants were obtained from the splitting of the cross peaks in the F_1 dimension by using a correction procedure described by Kay and Bax (1990). Water suppression was achieved by a DANTE pulse during the relaxation delay.

For determination of persistent amide protons, the ImmE3 sample in a buffered ^1H_2O was replaced by a buffered ^2H_2O by ultrafiltration using Centricon-3 at 4 °C. After 12 h of buffer exchange, the HOHAHA experiment was begun, and the duration of the measurement was approximately 14 h.

Results and Discussion

Identification of Spin System. Amino acid spin systems were identified by examining DQF-COSY spectra in ^2H_2O, HOHAHA spectra in ^1H_2O and ^2H_2O, and ^1H–^{15}N 2D HMQC-HOHAHA spectra. ImmE3 contains 84 amino acids, including three proline residues. Therefore, the fingerprint region of the DQF-COSY spectrum in ^1H_2O was expected to contain CαH–NH cross peaks which correspond to 81 amino acid residues. In the case of glycine residues, pairs of cross peaks are observed. In fact, the DQF-COSY spectrum in ^1H_2O contains cross peaks which correspond to 70 amino acid residues in fingerprint region (Figure 1). In HOHAHA spectrum recorded under the same conditions, 73 CαH–NH cross peaks were observed (data not shown). CβH–NH cross peaks indicate the four CαH–NH peaks lie under the water resonance and are obscured by presaturation at the water resonance. These four CαH–NH cross peaks were clearly visible in HOHAHA spectrum with the "jump-return" pulse (data not shown).

First, five of the six valines, two of the three isoleucines, five of the six leucines, two of the three lysines, and two threonines were identified in the HOHAHA and DQF-COSY spectra in ^2H_2O and ^1H_2O of the ImmE3 protein. And also 21 of 39 AMX spin systems were identified in the same spectra.

Five of the seven glycine residues in the ImmE3 protein could be identified from the presence of two fingerprint region COSY cross peaks along the same NH chemical shift axis and confirmed by CαH–Cα'H cross peaks in the HOHAHA spectrum in ^2H_2O, in which six of the seven glycine residues could be identified.

All three proline residues in the protein could be identified from the presence of the cross peaks of the side-chain protons

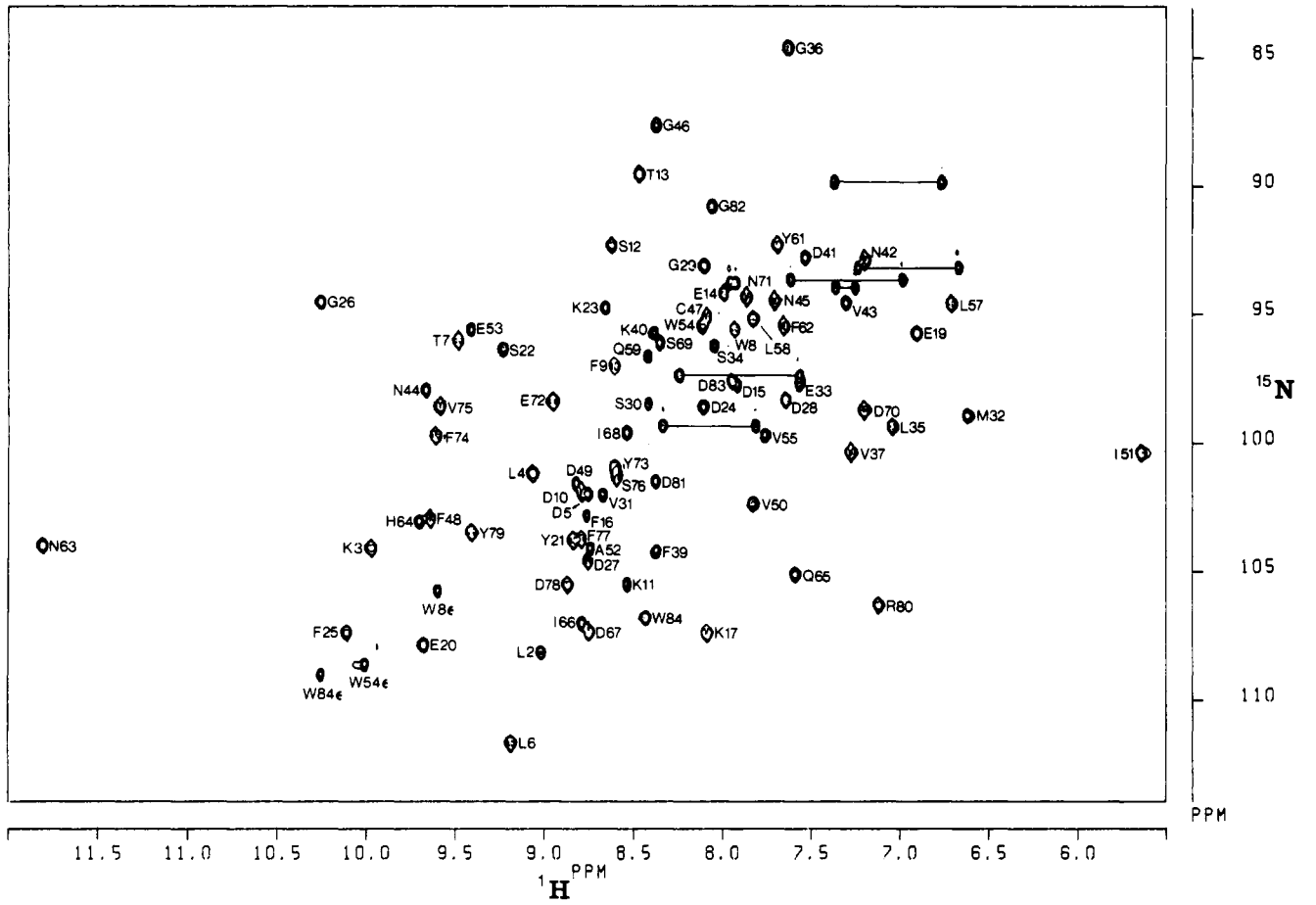

FIGURE 2: HMQC spectrum of the uniformly ^{15}N-labeled ImmE3 protein in $^{1}H_2O$ at pH 6.0 and 30 °C.

in the HOHAHA spectrum in $^{2}H_2O$ and the absence of the side-chain connectivities from amide protons in the HOHAHA spectrum in $^{1}H_2O$.

The ImmE3 protein contains many amino acids which have aromatic rings. Substantial overlapping of aromatic proton resonances made the assignment of those resonances difficult. The aromatic proton spin systems of two of the three tryptophane residues, two of the four tyrosine residues, and six of the eight phenylalanine residues were identified by examining DQF-COSY and HOHAHA spectra. In the NOESY spectra, the aromatic resonances of these residues were linked mainly to CβH protons of the same residues and to some NH or CαH protons.

The HMQC spectrum of the ImmE3 protein (Figure 2) was expected to contain 80 ^{1}H–^{15}N cross peaks except the three proline residues and the N-terminal glycine residue. Actually, 79 ^{1}H–^{15}N cross peaks, all three tryptophan indole amide protons, and all seven NH_2 groups of asparagine and glutamine residues were observed. Therefore, the number of the backbone amide proton resonances identified in the HMQC spectrum was larger than that in the DQF-COSY spectrum in $^{1}H_2O$.

Sequential Assignment. The sequential assignment of the ImmE3 protein spectrum was carried out by identifying through-bond and through-space connectivities (Wüthrich, 1986).

NOESY spectra were employed to observe through-space connectivities. In the sequential assignment procedure, the CαH–NH COSY cross peaks of glycine residues were chosen as starting points.

Only 21 of the residues in the ImmE3 were assigned in a straightforward manner using homonuclear 2D spectra. Those are peptide segments that contained the amino acid sequences Gly-1–Phe-9[2] and Gly-46–Ile-51, with strong NOEs between CαH(i) and NH(i+1), and Val-31–Gly-36, with weak NOEs between CαH(i) and NH(i+1) and strong NOEs between NH(i) and NH(i+1) (Figures 3 and 4). Three proline residues were assigned from the NOEs between the δ-protons of the proline residues and the α-protons of the preceding residues, and between the α-protons and the amide protons of the succeeding residues. The remaining residues were assigned by using a combination of homonuclear and heteronuclear 2D spectra.

In order to overcome substantial overlapping of resonances, the NOEs in the ^{1}H–^{15}N 2D HMQC-NOESY spectra were effectively used as well as usual ^{1}H–^{1}H NOESY spectra. As an example demonstration of the usefulness of the ^{1}H–^{15}N heteronuclear 2D spectra, we describe the case of Phe-74 and Val-75. In ^{1}H–^{1}H NOESY spectrum in $^{1}H_2O$, the amide proton chemical shifts of both residues were identical (9.59 ppm), and therefore, the sequential NOE of the CαH(i)–NH(i+1) overlapped the CαH(i)–NH(i) COSY peak (indicated with an arrow head in Figure 3). However, in ^{1}H–^{15}N 2D HMQC-NOESY spectra (not shown), each amide proton was separated according to its ^{15}N chemical shift (99.6 ppm for Phe-74 and 98.4 ppm for Val-75), and the strong NOE of CαH(i)–NH(i+1) was clearly identified.

Figure 4 shows the NH–NH region of the ^{1}H–^{15}N 2D HMQC-NOESY spectrum. By using this spectrum, the NH–NH NOEs were easily identified since there were no

[2] The residue numbers of Imm proteins are smaller by one here than in our previous papers (Masaki & Ohta, 1982, 1985; Akutsu et al., 1989; Masaki et al., 1991) because the final preparation of the protein lacks the N-terminal methionine.

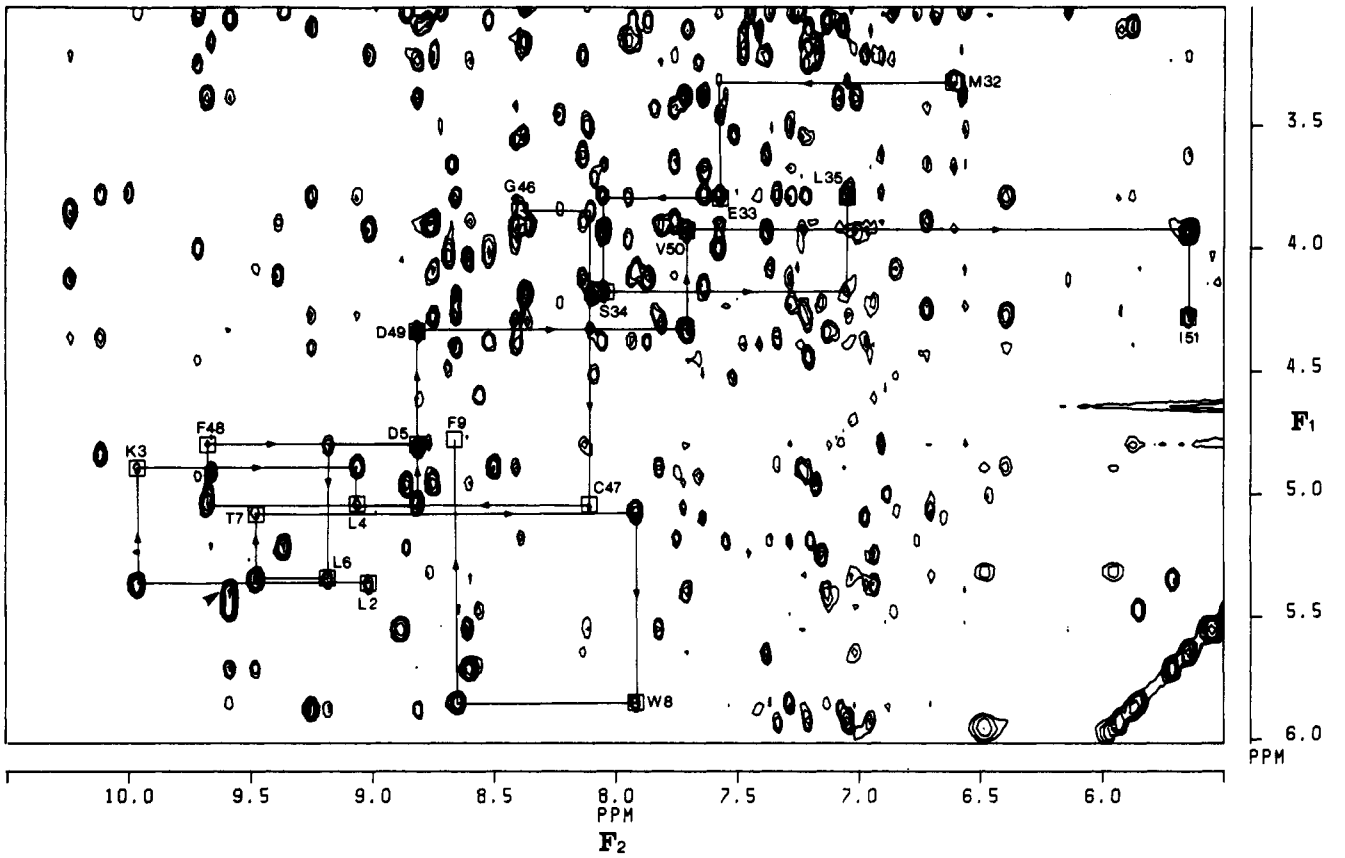

FIGURE 3: NH–aliphatic region of the 150-ms NOESY spectrum of the ImmE3 protein in ^1H_2O, at pH 6.0 and 30 °C. Stretches of CαH(i)–NH(i+1) connectivities extending over residues L2–F9, M32–L35, and G46–I51 are indicated by continuous lines. Boxes indicate the positions of intraresidual CαH–NH NOE cross peaks. An arrow head indicates the sequential NOE between the CαH proton of Phe-74 and the NH of Val-75.

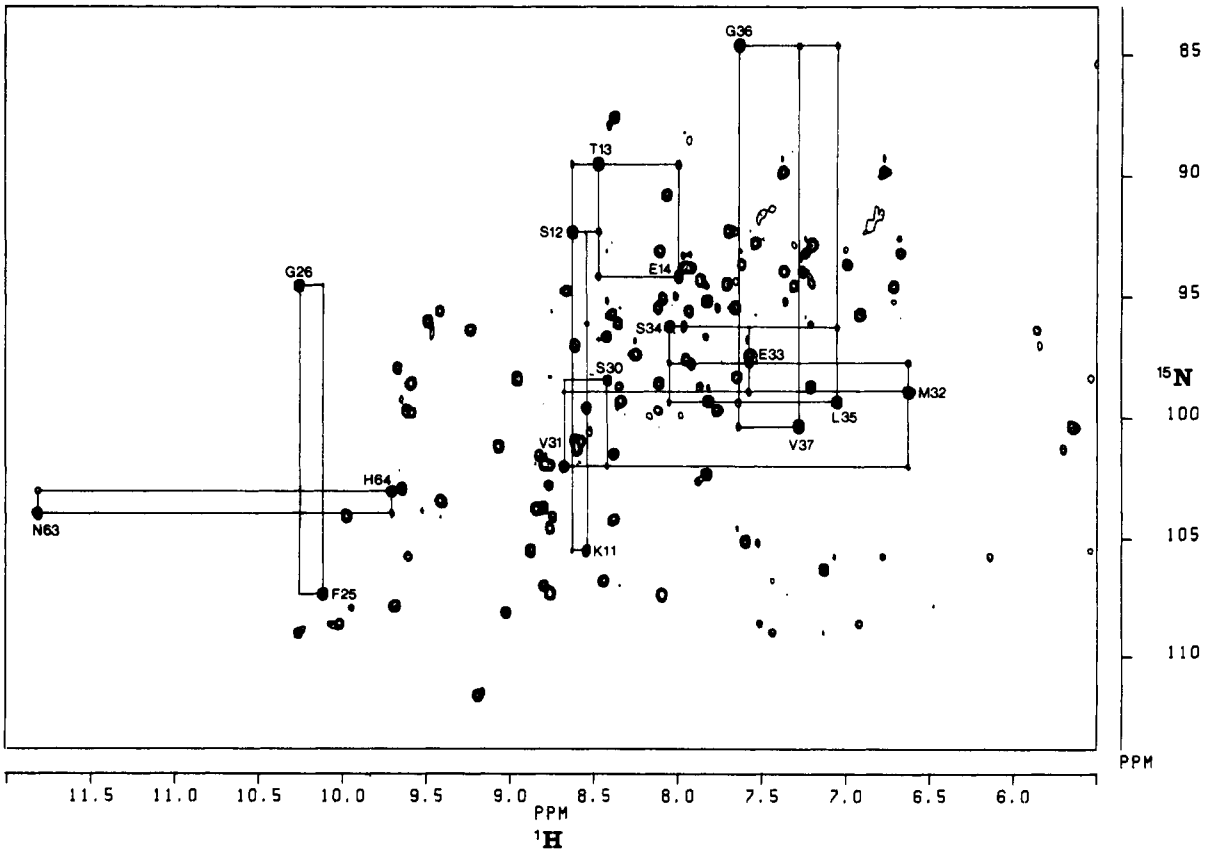

FIGURE 4: Amide proton region of the HMQC-NOESY spectrum of the ImmE3 protein, with a mixing time of 100 ms, at pH 6.0 and 30 °C. Stretches of NH(i)–NH(i+1) connectivities extending over residues K11–E14, F25–G26, V31–V37, and N63–H64 are indicated by continuous lines.

FIGURE 5: Summary of the short-range NOE connectivities along with the amino acid sequence of the immE3 protein. The $^3J_{NH\alpha}$ coupling constants larger than or equal to 8 Hz of the residues are indicated by open circles.

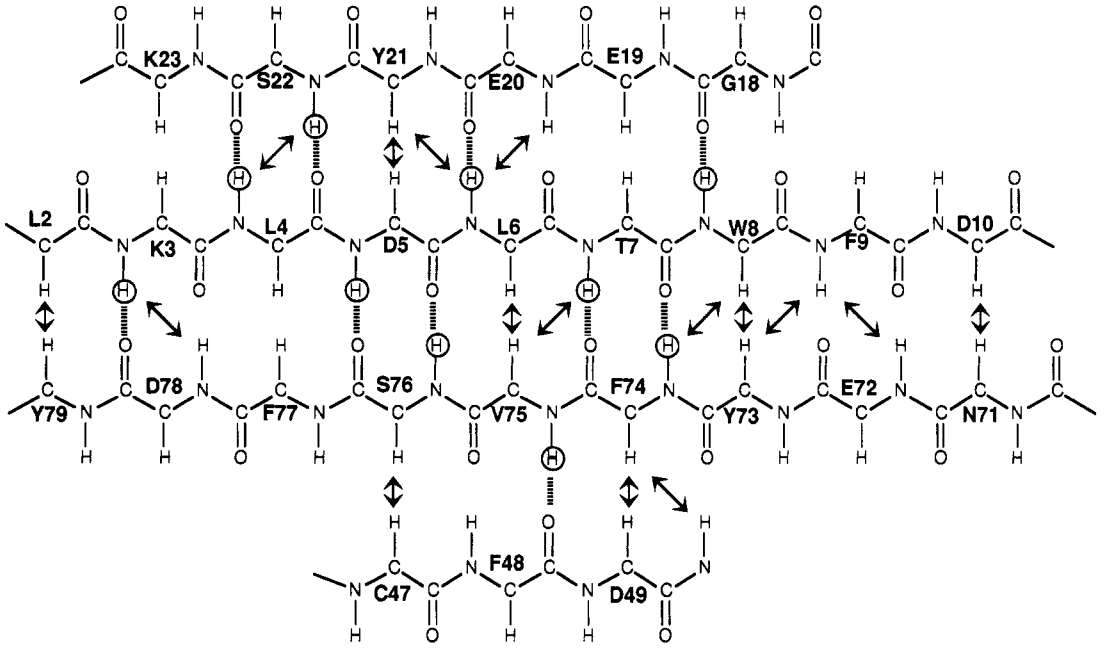

FIGURE 6: Schematic diagram of the region of antiparallel β-sheet in the ImmE3 protein. Dashed lines show hydrogen bonds indicated from slow exchange rates of the amide protons which are indicated by circles.

aromatic proton resonances which were observed in the ^1H–^1H NOESY spectrum in ^1H_2O. Several consecutive stretches were indicated, namely, over residues 12–15, 31–38, 58–60, and 69–72. And some other NOEs of NH(i)–NH(i+1) were observed in this spectrum (Figure 4). Side-chain proton resonances were assigned using the DQF-COSY spectra in ^2H_2O and the HOHAHA spectra in ^2H_2O and in ^1H_2O. As a result of the spectral analysis described above, the complete assignments of observable ^{15}N, NH proton, CαH proton, and side-chain proton resonances were determined as shown in Table I. Unambiguous assignments were not obtained for the Gly-18 protons due to the missing of its resonance peaks in both homonuclear and heteronuclear spectra. It is worth pointing out that two amino acid residues, Asn-63 and Ile-51, exhibit extremely high- or low-field shifts of the NH proton resonances at 11.82 and 5.65 ppm, respectively. These resonance positions are downfield-shifted by 3.07 ppm (Asn-63 NH) and upfield-shifted by 2.54 ppm (Ile-51 NH) with respect to their random coil positions. For Ile-51 NH it is most likely due to close special proximity of aromatic rings. The DQF-COSY spectrum in ^1H_2O of the nonlabeled protein purified from pUIE3 was the same as that from pSH312 (data not shown).

Secondary Structure. Qualitative interpretation of the short-range NOEs including the NH, CαH, and CβH protons is summarized along with the amino acid sequence in Figure 5.

The NOESY spectrum of ImmE3 exhibits a number of long-range CαH–NH, NH–NH, and CαH–CαH NOEs which identify β-sheet structures (Yamasaki et al., 1989).

Table I: ^{1}H and ^{15}N Chemical Shift (ppm) of the ImmE3 Protein, at pH 6.0 and 30 °C[a]

residue	^{15}N	NH	αH	βH	γH	δH	others
Gly-1			3.20, 3.93				
Leu-2	108.0	9.01	5.25	1.73, 2.03	1.51	0.79, 1.23	
Lys-3	104.0	9.96	4.89	1.10, 1.76	1.30	0.88	
Leu-4	100.9	9.05	5.04	1.67, 1.93	0.89	0.74	
Asp-5	101.8	8.81	4.03	2.43			
Leu-5	101.0	9.18	5.33	1.74, 2.04	0.83		δCH$_3$ 0.05, 0.62
Thr-7	95.8	9.47	5.08	4.04	1.13		
Trp-8	95.5, 105.5 (Nε)	7.93	5.85	1.63, 2.83			2H 6.14; 4 H 7.02; 5H 6.00; 6H 6.51; 7H 6.89
Phe-9	96.9	8.65	4.80	2.64, 2.79			2,6H 7.29; 3,5H 7.38; *
Asp-10	101.8	8.77	4.75	3.08			
Lys-11	105.4	8.60	4.04	1.82, 1.63	1.35, 1.45	1.55	εH 2.87
Ser-12	92.2	8.68	4.48	3.98, 4.04			
Thr-13	89.3	8.52	4.39	3.67, 1.20			
Glu-14	94.1	7.86	4.11	2.05, 2.20	2.35		
Asp-15	97.6	7.91	4.70	2.48, 2.60			
Phe-16	102.7	8.71	3.51	3.05, 2.70			2,6H 6.58; 3,5H 6.86; 4H 6.82
Lys-17	107.2	8.11	4.11	1.44, 1.17	1.33	1.66	εH 2.97
Gly-18	*	*	*				
Glu-19	95.6	6.68	5.01	1.70, 1.86	2.20, 2.80		
Glu-20	107.7	9.66	4.61	2.23, 2.48	2.66, 2.79		
Tyr-21	103.6	8.80	5.86	2.88, 3.10			2,6H 7.08; 3,5H 6.89
Ser-22	96.2	9.25	4.39	2.56, 2.62			
Lys-23	94.8	8.64	4.19	*	*	*	*
Asp-24	98.4	8.10	4.48	2.76, 2.14			
Phe-25	107.1	10.12	4.36	2.86, 1.74			2,6H 7.33; 3,5H 5.96; 4H 7.05
Gly-26	94.5	10.24	3.86, 4.11				
Asp-27	104.4	8.74	5.11	2.95, 2.58			
Asp-28	98.2	7.64	4.52	3.39, 2.70			
Gly-29	93.0	8.08	2.98, 3.70				
Ser-30	98.3	8.39	3.80	3.50			
Val-31	101.8	8.66	3.67	1.32	0.48, 0.19		
Met-32	98.9	6.61	3.32	1.39, 1.57	1.79, 2.35		
Glu-33	102.7	7.58	3.76	1.91	2.23		
Ser-34	96.0	8.05	4.17	3.92, 3.95			
Leu-35	99.3	7.05	3.76	0.39, 1.20	1.48		δCH$_3$ −0.13, 0.10
Gly-36	87.4	7.63	3.67, 4.14				
Val-37	100.3	7.29	4.21	1.21	0.48, 0.22		
Pro-38			4.18	1.76, 2.29	1.89, 2.01	3.84, 3.46	
Phe-39	102.3	8.30	4.15	3.15			*
Lys-40	95.6	8.38	3.54	1.73, 1.63	1.37, 1.20	1.51	εH 2.88
Asp-41	92.7	7.52	4.54	2.39, 2.76			
Asn-42	92.8	7.20	5.18	2.32, 2.67			
Val-43	94.5	7.29	4.76	1.86	0.64, −0.38		
Asn-44	97.8	9.68	4.92	3.14, 2.48			
Asn-45	94.3	7.74	5.18	2.54, 2.86			
Gly-46	87.4	8.38	3.84, 4.30				
Cys-47	95.0	8.10	5.04	2.15, 2.79			
Phe-48	102.8	9.68	4.82	3.39			2,6H 7.75; 3,5H 7.57; *
Asp-49	101.3	8.81	4.32	2.36, 2.44			
Val-50	102.2	7.70	3.92	1.98	0.79, 0.95		
Ile-51	100.3	5.65	4.30	1.85	0.62		δCH$_3$ −0.37
Ala-52	104.0	8.72	3.89	1.39			
Glu-53	95.5	9.40	4.10	2.10	2.34, 2.45		
Trp-54	95.3, 108.3 (Nε)	8.12	4.82	2.20, 3.60			2H 6.82; 4H 7.52; 5H 7.10; 6H 7.03; 7H 7.40
Val-55	99.5	7.77	3.41	2.39	0.88, 0.92		
Pro-56			4.46	1.62, 2.28	1.95, 2.01	3.89, 3.64	
Leu-57	94.5	6.72	4.22	1.89, 1.38	1.76		δCH$_3$ 0.85, 0.91
Leu-58	95.1	7.84	4.66	1.62	1.58		δCH$_3$ 1.92
Gln-59	96.5	8.40	3.88	1.40	*		
Pro-60			4.23	1.60, 1.71	2.96	3.58	
Tyr-61	92.1	7.70	4.45	2.48, 3.10			2,6H 10.52; 3,5H 10.28
Phe-62	95.3	7.66	4.91	2.35, 3.24			2,6H 7.24; 3,5H 7.43; *
Asn-63	103.9	11.82	4.45	2.74, 2.95			
His-64	102.9	9.71	3.97	2.42, 3.00			
Gln-65	105.0	7.57	3.99	1.63	2.08		
Ile-66	106.9	8.76	2.95	1.26	0.17		γCH$_3$ −0.30; δCH$_3$ 0.46
Asp-67	107.1	8.75	4.92	2.95, 2.26			
Ile-68	99.5	8.49	4.89	2.08	1.79, 1.51		γCH$_3$ −1.10; δCH$_3$ −0.20
Ser-59	95.9	8.41	4.39	3.91, 3.98			
Asp-70	98.6	7.25	4.89	2.45, 2.67			
Asn-71	94.1	7.82	5.54	2.20, 2.54			
Glu-72	98.2	8.88	4.61	1.79, 2.01	2.16, 2.20		
Tyr-73	100.7	8.55	5.48	2.73			2,6H 6.89; 3,5H 6.82
Phe-74	99.6	9.59	5.39	2.93, 3.04			2.6H 7.15; *
Val-75	98.4	9.59	5.70	1.79	0.73, 0.98		
Ser-76	101.1	8.60	4.96	3.89, 4.04			
Phe-77	103.8	8.95	4.96	3.17, 3.22			

Table I (Continued)

residue	^{15}N	NH	αH	βH	γH	δH	others
Asp-78	105.4	8.85	5.20	3.04			
Tyr-79	103.3	9.36	5.26	2.64, 2.85			2,6H 6.95; 3,5H 6.98; *
Arg-80	106.1	7.16	4.23	0.62, 0.69	0.98, 1.17	2.47	
Asp-81	101.3	8.48	4.28	3.13, 2.98			
Gly-82	90.7	8.05	3.79, 3.95				
Asp-83	97.5	7.95	4.64	2.45, 2.64			
Trp-84	106.7, 109.0 (Nε)	8.39	4.39	3.11, 3.21			2H 7.39; *

[a] An asterisk indicates that the resonance of the proton has not been identified.

These results imply a four-stranded antiparallel β-sheet formed by residues 2–10, 18–23, 47–49, and 71–79, as illustrated in Figure 6 with interstrand NOEs. Furthermore, this β-sheet structure was confirmed by the $^3J_{HN\alpha}$ coupling constants larger than 8 Hz (Figure 5) of the residues in the sheet.

The exchange of an NH proton is inhibited by the formation of a hydrogen bond, often giving another line of evidence of a secondary structure element, such as an α-helix or a β-sheet (Wüthrich, 1986). Fourteen CαH–NH cross peaks were observed in the HOHAHA spectrum of the ImmE3 sample prepared by ultrafiltration with buffered ^2H_2O for the measurement of the exchange rates of the amide protons as described under Materials and Methods. This result suggests the inhibition of exchange of these NH protons and, consequently, their involvement in hydrogen bonds. These findings are consistent with the antiparallel β-sheet proposed above.

The four β-strands are connected by a short loop (11–17) and two long loops (24–46 and 50–70). Furthermore, we found that there is only one short α-helix extending over the residues 31–37, from stretches of strong NH(i)–NH(i+1) connectivities in conjunction with diagnostic CαH(i)–NH(i+3) and CαH(i)–CαH(i+4) NOEs. This short α-helix is located at the center of the long loop linking two β-strands of residues 18–23 and 47–49.

Specificity Determination of ImmE3. ImmE3 and ImmE6 are extensively homologous proteins, whereas they show distinct immunity specificities (Akutsu et al., 1989). Our previous experiment demonstrated that an ImmE6 mutant with a single replacement of Trp-47 by Cys-47 of the ImmE3-type acquires the immunity to E3. Furthermore, characterization of the chimeric genes between *immE3* and *immE6* showed that (1) Cys-47 is in fact critically important for the Imm3 specificity, (2) Asp-15 or Glu-19 of ImmE3 is a subdeterminant of the ImmE3 specificity, and (3) His-5, or Ile-6, and Trp-47 of ImmE6 are needed for the full ImmE6 specificity (Masaki et al., 1991). Considering that Asp-15 of ImmE3 has a homologous counterpart, Glu-15 in ImmE6, and also that Leu-6 of ImmE3 has Ile-6 in ImmE6, our genetic study predicted three important residues, 5, 19, and 47, in the specificity determinations of the ImmE3 and ImmE6 proteins.

Interestingly, these three sites are all included in the β-sheet of ImmE3 and also protrude their side groups into the same side of the β-sheet (Figure 6). Alternate residues along the amino acid sequence in a β-sheet represent the same side of the sheet. Around the above three important hydrophilic residues, hydrophilic residues are evidently located on the same side and hydrophobic ones are on the other side of the β-sheet (Figure 6). These findings result in a model in which only one side of the β-sheet is exposed to the solution, allowing its rather small area to form the specificity determinant of ImmE3.

This has to await a full structural characterization of the protein based on the NOEs between residues distant in the sequence, which is in progress in our group. Many Imm proteins with various specificities that we obtained are promising in the complete description of the protein–protein interaction between colicins and Imm proteins by the genetic and physicochemical experiments.

Acknowledgments

We thank Kazuhiko Yamasaki and Yutaka Ito for continuous help and stimulating discussions.

Supplementary Material Available

A HOHAHA spectrum in ^1H_2O, HOHAHA, DQF-COSY, and NOESY spectra in ^2H_2O for the sequential assignment, a HOHAHA spectrum in ^2H_2O for persistent amide protons, and a HMQC-J spectrum (6 pages). Ordering information is given on any current masthead page.

References

Akutsu, A., Masaki, H., & Ohta, T. (1989) *J. Bacteriol. 171*, 6430–6436.

Arrowsmith, C. H., Pachter, R., Altman, R. B., Iyer, S. B., & Jardetzky, O. (1990) *Biochemistry 29*, 6332–6341.

Bax, A., & Davis, D. G. (1985) *J. Magn. Reson. 65*, 355–360.

Bax, A., Griffey, R. H., & Hawkins, B. L. (1983) *J. Am. Chem. Soc. 105*, 7188–7190.

Bax, A., Sklenar, V., Clore, G. M., & Gronenborn, A. M. (1987) *J. Am. Chem. Soc. 109*, 6511–6513.

Boon, T. (1971) *Proc. Natl. Acad. Sci. U.S.A. 68*, 2421–2425.

Bowman, C. M., Sidikaro, J., & Nomura, M. (1971) *Nature (London) New Biol. 234*, 133–137.

Braunschweiler, L., & Ernst, R. R. (1983) *J. Magn. Reson. 53*, 521–528.

Buxton, R. S. (1971) *Mol. Gen. Genet. 113*, 154–156.

Davis, D. G., & Bax, A. (1985) *J. Am. Chem. Soc. 107*, 2821–2822.

de Graaf, F. K., Niekus, H. G. D., & Klootwijk (1973) *FEBS Lett. 35*, 161–165.

Dekker, N., Peters, A. R., Slotboom, A. J., Boelens, R., Kaptein, R., & de Haas, G. (1991) *Biochemistry 30*, 3135–3147.

DiMasi, D. R., White, J. C., Schnaitman, C. A., & Bradbeer, C. (1973) *J. Bacteriol. 115*, 506–513.

Driscoll, P. C., Clore, G. M., Marion, D., Wingfield, P. T., & Glushka, J., & Cowburn, D. (1987) *J. Am. Chem. Soc. 109*, 7879–7881.

Fairbrother, W. J., Cavanagh, J., Dyson, H. J., Palmer, A. G., III, Sutrina, S. L., Reizer, J., Saier, M. H., Jr., & Wright, P. E. (1991) *Biochemistry 30*, 6896–6907.

Glushka, J., & Cowburn, D. (1987) *J. Am. Chem. Soc. 109*, 7879–7881.

Gronenborn, A. M. (1990) *Biochemistry 29*, 3542–3556.

Gronenborn, A. M., Bax, A., Wingfield, P. T., & Clore, G. M. (1989) *FEBS Lett. 243*, 93–98.

Hershman, H. R., & Helinski, D. R. (1967) *J. Biol. Chem. 242*, 5360–5368.

Ikura, M., Kay, L. E., & Bax, A. (1990) *Biochemistry 29*, 4659–4667.

Jakes, K. S., & Zinder, N. D. (1974) *Proc. Natl. Acad. Sci. U.S.A. 74*, 3380-3384.
Jeener, J., Meier, B. H., Bachmann, P., & Ernst, R. R. (1979) *J. Chem. Phys. 71*, 4546-4533.
Kay, L. E., & Bax, A. (1990) *J. Magn. Reson. 86*, 110-126.
MacIntosh, L. P., Wand, A. J., Lowry, D. F., Redfield, A. G., & Dahlquist, F. W. (1990) *Biochemistry 29*, 6341-6362.
Macura, S., Huang, Y., Suter, D., & Ernst, R. R. (1981) *J. Magn. Reson. 43*, 259-281.
Marion, D., & Wüthrich, K. (1983) *Biochem. Biophys. Res. Commun. 113*, 967-974.
Masaki, H., & Ohta, T. (1982) *FEBS Lett. 149*, 129-132.
Masaki, H., & Ohta, T. (1985) *J. Mol. Biol. 182*, 217-227.
Masaki, H., Akutsu, A., & Ohta, T. (1991) *Gene 107*, 133-138.
Messing, J., (1983) *Methods Enzymol. 101*, 20-78.
Mochitate, K., Suzuki, K., & Imahori, K. (1981) *J. Biochem. (Tokyo) 89*, 1609-1618.
Mueller, L. (1979) *J. Am. Chem. Soc. 101*, 4481-4484.
Ohno, S., & Imahori, K. (1978) *J. Biochem. (Tokyo) 84*, 1637-1640.
Ohno-Iwashita, Y., & Imahori, K. (1980) *Biochemistry 19*, 652-659.
Piatini, U., Sørenson, O. W., & Ernst, R. R. (1982) *J. Am. Chem. Soc. 104*, 7310-7311.
Plateau, P., & Gueron, M. (1982) *J. Am. Chem. Soc. 104*, 7310-7311.
Pugsley, A. P., & Oudega, B. (1987) *Plasmids: A Practical Approach*, IRL Press, Oxford.
Rance, M., Sørensen, O. W., Bodenhausen, G., Wagner, G., Ernst, R. R., & Wüthrich, K. (1983) *Biochem. Biophys. Res. Commun. 117*, 479-485.
Redfield, A. G. (1983) *Chem. Phys. Lett. 96*, 537-540.
Redfield, A. G., & Kuntz, S. D. (1975) *J. Magn. Reson. 19*, 250-254.
Skelnar, V., & Bax, A. (1987) *J. Magn. Reson. 71*, 379-383.
Suzuki, K., & Imahori, K. (1978) *J. Biochem. (Tokyo) 84*, 1031-1039.
Toba, M., Masaki, H., & Ohta, T. (1986) *J. Biochem. (Tokyo) 99*, 591-596.
Torchia, D. A., Sparks, S. W., & Bax, A. (1989) *Biochemistry 28*, 5509-5524.
Wang, J., Hinck, A. P., Loh, S. N., & Markley, J. L. (1990) *Biochemistry 29*, 102-113.
Wüthrich, K. (1986) *NMR of Proteins and Nucleic Acids*, Wiley, New York.
Yamasaki, K., Kawai, G., Ito, Y., Muto, Y., Fujita, J., Miyazawa, T., Nishimura, S., & Yokoyama, S. (1989) *Biochem. Biophys. Res. Commun. 162*, 1054.
Yamasaki, K., Muto, Y., Ito, Y., Wälchili, M., Miyazawa, T., Nishimura, S., & Yokoyama, S. (1992) *J. Biomol. NMR* (in press).
Yanisch-Perron, C., Vieira, J., & Messing, J. (1985) *Gene 33*, 103-119.

Fluorenyl Fatty Acids as Fluorescent Probes for Depth-Dependent Analysis of Artificial and Natural Membranes†

Anil K. Lala* and Vishwanath Koppaka
Biomembrane Lab, Department of Chemistry, Indian Institute of Technology Bombay, Powai, Bombay 400076, India
Received October 2, 1991; Revised Manuscript Received March 18, 1992

ABSTRACT: The main objective of depth-dependent fluorescent probes is to provide information at a distinct position in the membrane hydrophobic core. We report here a series of fluorenyl fatty acids which can probe both artificial and natural membranes at different depths. Long-chain acids (C4, C6, and C8) are attached to fluorene chromophore on one side, and a hydrophobic tail (C4) is attached on the other side, so that on incorporation in membranes the carboxyl end of the molecule is oriented toward the membrane–water interface and the hydrophobic tail points toward the membrane interior. These acids can be readily partitioned into membranes. The disposition of these fluorenyl fatty acids in membranes was studied by fluorescence quenching using iodide as a water-soluble and 9,10-dibromostearic acid as a lipid-soluble quencher. The results obtained indicate that attachment of a hydrophobic tail is essential for effective alignment of depth-dependent fluorescent probes. The length of the hydrophobic tail was varied and an *n*-butyl chain was found to be most effective. In all cases, the compounds with a hydrophobic tail were found to be probing the membrane deeper than their counterparts with no hydrophobic tail. Further, the compounds with hydrophobic tails were more strongly immobilized in the membrane as indicated by fluorescence polarization studies. However, the effect of such a tail varied with membrane type. Thus in artificial membranes an *n*-butyl chain was found to be extremely important for effective monitoring by shallow probes like 4-(2′-fluorenyl)butyric acid, whereas in erythrocyte ghost membranes the same *n*-butyl tail was found to be more desirable for deeper probes like 8-(2′-fluorenyl)octanoic acid. The general molecular design strategy reported here can be extended to other fluorescent probes and photoactivable reagents for depth-dependent analysis of membranes.

The main objective of depth-dependent analysis of membranes is to provide information at different depths. Fluorescent probes have been frequently used toward this end (Blatt & Sawyer, 1985). Both fluorescent fatty acids and phospholipids have been used in this context. The most notable in this class have been the *n*-anthroyloxy fatty acids (Thulborn & Sawyer, 1978), pyrenyl fatty acids (Waka et al., 1980; Jones & Lentz, 1986), and anthracene fatty acids (de Bony & To-

† This work was supported by a grant-in-aid from the Department of Science and Technology, Delhi, India.
* Author to whom correspondence should be addressed.

0006-2960/92/0431-5586$03.00/0